Accumulation of Mad2–Cdc20 complex during spindle checkpoint activation requires binding of open and closed conformers of Mad2 in *Saccharomyces cerevisiae*

Luigi Nezi,[1] Giulia Rancati,[2] Anna De Antoni,[1] Sebastiano Pasqualato,[1,3] Simonetta Piatti,[2] and Andrea Musacchio[1,3]

[1]Department of Experimental Oncology, European Institute of Oncology, 20141 Milan, Italy
[2]Department of Biotechnology and Bioscience, University of Milan-Bicocca, 20126 Milan, Italy
[3]The Fondazione Italiana per la Ricerca sul Cancro Institute of Molecular Oncology Foundation, 20139 Milan, Italy

The spindle assembly checkpoint (SAC) coordinates mitotic progression with sister chromatid alignment. In mitosis, the checkpoint machinery accumulates at kinetochores, which are scaffolds devoted to microtubule capture. The checkpoint protein Mad2 (mitotic arrest deficient 2) adopts two conformations: open (O-Mad2) and closed (C-Mad2). C-Mad2 forms when Mad2 binds its checkpoint target Cdc20 or its kinetochore receptor Mad1. When unbound to these ligands, Mad2 folds as O-Mad2. In HeLa cells, an essential interaction between C- and O-Mad2 conformers allows Mad1-bound C-Mad2 to recruit cytosolic O-Mad2 to kinetochores. In this study, we show that the interaction of the O and C conformers of Mad2 is conserved in *Saccharomyces cerevisiae*. *MAD2* mutant alleles impaired in this interaction fail to restore the SAC in a *mad2* deletion strain. The corresponding mutant proteins bind Mad1 normally, but their ability to bind Cdc20 is dramatically impaired in vivo. Our biochemical and genetic evidence shows that the interaction of O- and C-Mad2 is essential for the SAC and is conserved in evolution.

Introduction

The spindle assembly checkpoint (SAC) is activated during each mitosis to monitor the attachment of sister chromatids to the spindle (Musacchio and Hardwick, 2002). Upon biorientation of all sister chromatid pairs, the SAC is switched off, and anaphase ensues. SAC components such as products of the *MAD* (mitotic arrest deficient) and *BUB* (budding uninhibited by benzymidazole) genes are recruited to kinetochores in prometaphase, where they monitor the attachment of microtubules and the tension that builds up between bipolarly attached sister chromatids (Cleveland et al., 2003).

Critical to the SAC is the interaction of Mad2 with Cdc20 (Hwang et al., 1998; Kim et al., 1998). The latter is a positive regulator of the anaphase-promoting complex or cyclosome, whose function is required for progression into anaphase (Peters, 2002). In mitosis, Mad2 is continuously recruited to kinetochores and is released from these structures in a form that binds Cdc20 and sequesters it in an inactive form (Howell et al., 2000, 2004; Shah et al., 2004). When all chromosomes are aligned on the metaphase plate, Cdc20 is reactivated, and the consequent activation of the anaphase-promoting complex or cyclosome triggers anaphase.

Mad1 is required to recruit Mad2 at kinetochores and for efficient formation of the Mad2–Cdc20 complex. Two models have been proposed to explain the role of Mad1 in eliciting the formation of the Mad2–Cdc20 complex (for review see Hagan and Sorger, 2005; Hardwick, 2005; Nasmyth, 2005). The Mad2 exchange model proposes that Mad1 recruits open Mad2 (O-Mad2) at the kinetochore and changes its conformation from O-Mad2 to closed Mad2 (C-Mad2). C-Mad2 then dissociates from Mad1 and binds Cdc20. This model depicts Mad1 as a catalyst of the conversion of O-Mad2 into C-Mad2, which, in turn, is required for Mad2 to bind Cdc20 (Luo et al., 2004). However, the Mad2 exchange model is weakened by structural observations, indicating that Mad1 and Cdc20 bind the same pocket of Mad2. In the frame of the Mad2 exchange model, this

L. Nezi and G. Rancati contributed equally to this paper.

Correspondence to Andrea Musacchio: andrea.musacchio@ifom-ieo-campus.it; or Simonetta Piatti: simonetta.piatti@unimib.it

G. Rancati's present address is Stowers Institute for Medical Research, Kansas City, MO 64110.

Abbreviations used in this paper: GSH, glutathione–Sepharose; IP, immunoprecipitation; MAD, mitotic arrest deficient; SAC, spindle assembly checkpoint; SEC, size-exclusion chromatography.

The online version of this article contains supplemental material.

The Journal of Cell Biology, Vol. 174, No. 1, July 3, 2006 39–51
http://www.jcb.org/cgi/doi/10.1083/jcb.200602109

implies that Mad1 and Cdc20 compete for Mad2 binding, which would rule out a role for Mad1 as a direct activator of Mad2 for Cdc20 binding (De Antoni et al., 2005a).

The Mad2 template model resolves this difficulty by incorporating a remarkable property of Mad2: the ability of its two conformers, O- and C-Mad2, to bind each other in a conformational dimer (Luo et al., 2004; De Antoni et al., 2005a,b). The model proposes that the kinetochore receptor of O-Mad2 is a tight complex between Mad1 and C-Mad2 (the Mad1–Mad2 core complex; Sironi et al., 2002; De Antoni et al., 2005a). Mad1 provides this very sturdy complex with an N-terminal kinetochore-targeting domain and a C-terminal Mad2-binding motif. The latter generates a stable form of kinetochore-bound C-Mad2 that acts as the O-Mad2 receptor. In the Mad2 template model, the C-Mad2 pool bound to Mad1 at the kinetochore and the O-Mad2 pool in the cytosol are distinct and nonexchanging. Thus, the model does not imply that Mad1 and Cdc20 compete for Mad2 binding, resolving the contradictions of the Mad2 exchange model (De Antoni et al., 2005a; Nasmyth, 2005). Furthermore, the Mad2 template model provides a useful molecular framework to understand the existence of two distinct kinetochore pools of Mad2 revealed by FRAP (Shah et al., 2004). Specifically, ∼50% of kinetochore Mad2 exchanges rapidly at unattached kinetochores, whereas a remaining 50% of Mad2 is stably bound (Shah et al., 2004). The observation that Mad1 is also stable at unattached kinetochores (Howell et al., 2004; Shah et al., 2004) prompted the suggestion that a stable Mad1–Mad2 complex might be involved in the recruitment of a cycling cytosolic fraction of Mad2 (Shah et al., 2004). When combined with the molecular information of the Mad2 template model, these experiments suggest that the kinetochore cycle of Mad2 represents the rate of transformation of O-Mad2 into Cdc20-bound C-Mad2.

An implication of the Mad2 template model is that the interaction of the O and C conformers of Mad2 facilitates the conversion of cytosolic O-Mad2 to Cdc20-bound C-Mad2. This might occur via mass action after concentrating O-Mad2 and Cdc20 at kinetochores or possibly catalytically by facilitating the structural conversion of Mad2 from O- to C-Mad2. Although initial evidence has been provided indicating that the interaction of O- and C-Mad2 is important for the SAC in HeLa cells (De Antoni et al., 2005a,b), a more rigorous analysis is required. We studied the properties of the *Saccharomyces cerevisiae*'s homologue of Mad2 (ScMad2), asking whether we could identify the biochemical and genetic properties supporting the Mad2 template model in mammalian cells. Our new genetic and biochemical evidence is completely consistent with the Mad2 template model.

Results

MAD2 mutants impaired in the open–closed interaction do not restore the SAC in a *mad2Δ* strain

Two mutants of HsMad2 (the point mutant Arg133-Ala and the double point mutant Arg133-Glu/Gln134-Ala, abbreviated as $Mad2^{RA}$ and $Mad2^{RQEA}$, respectively) are impaired in the interaction between O- and C-Mad2 (Sironi et al., 2001; De Antoni et al., 2005a,b). The residues map to a solvent-exposed surface of Mad2, and their mutation does not significantly affect Mad2's structural stability (De Antoni et al., 2005a). The choice of using the $Mad2^{RQEA}$ double mutant rather than the double alanine point mutant $Mad2^{RQAA}$ arose because the recombinant form of the latter was largely insoluble, whereas good yields of $Mad2^{RQEA}$ could be recovered from the soluble bacterial fraction (De Antoni et al., 2005a). Both $Mad2^{RA}$ and $Mad2^{RQEA}$ bind Mad1 and Cdc20 in vitro with identical affinity relative to wild-type Mad2 ($Mad2^{wt}$; Sironi et al., 2001, 2002; De Antoni et al., 2005a). Although the overexpression of $Mad2^{RA}$ and $Mad2^{RQEA}$ elicits a mitotic arrest (Sironi et al., 2001; De Antoni et al., 2005a), near-physiological concentrations of these mutant proteins were unable to support the SAC in HeLa cells concomitantly depleted of $Mad2^{wt}$ by RNAi (De Antoni et al., 2005a).

To carry out more rigorous complementation experiments, we examined the effects of equivalent *MAD2* mutations on the SAC in *S. cerevisiae*. Arg133 and Gln134 of HsMad2 are conserved in evolution. The equivalent yeast residues are Arg126 and Gln127 (Aravind and Koonin, 1998). We assayed the ability of $ScMad2^{wt}$, ScMad2-Arg126-Ala ($ScMad2^{RA}$), and ScMad2-Gln127-Ala ($ScMad2^{QA}$) to restore the SAC deficiency caused by deleting *MAD2* in *S. cerevisiae*. Cells arrested in G1 with α factor were released in the cell cycle in the presence of nocodazole to activate the SAC. To assess SAC proficiency, we monitored (1) the ability to arrest in mitosis and to prevent re-replication, (2) the lack of rebudding, and (3) the retention of sister chromatid cohesion. Wild-type cells completed DNA replication at ∼60 min after release from the G1 block in nocodazole and arrested as budded cells with 2C DNA content without rebudding or separating the sister chromatids (Fig. 1, A and B), which is indicative of an active SAC. Conversely, *mad2Δ* cells were unable to arrest, lost sister chromatid cohesion, rebudded, and re-replicated their DNA, which is indicative of a disrupted SAC.

To test the complementation potential of different *MAD2* alleles, we integrated wild-type and mutant *MAD2* alleles at the *LEU2* locus of the *mad2Δ* strain. $Mad2^{wt}$, $Mad2^{RA}$, and $Mad2^{QA}$ were expressed at similar levels, and their expression was essentially identical to that of endogenous Mad2 (see Fig. 7). The expression of $Mad2^{wt}$ in the *mad2Δ* strain fully restored the SAC (Fig. 1, A and B). However, the expression of $Mad2^{RA}$ and $Mad2^{QA}$ failed to complement the lack of *MAD2*. Cells expressing these proteins underwent sister chromatid separation, rebudding, and re-replication with timings that were very similar to those displayed by the bare *mad2Δ* strain.

The O and C conformers of ScMad2 form a conformational dimer

These results demonstrate that the ScMad2 surface containing Arg126 and Gln127 is essential for the SAC, confirming our previous observations in HeLa cells (De Antoni et al., 2005a). The residues equivalent to Arg126 and Gln127 (Arg133 and Gln134) in HsMad2 are part of an interface that mediates the

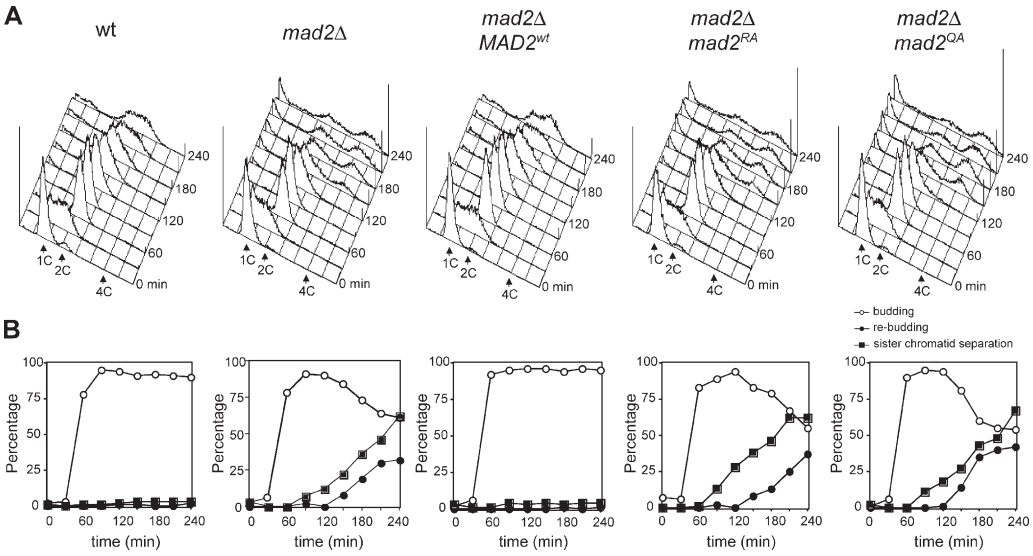

Figure 1. **The *mad2*^{RA} and *mad2*^{QA} point mutant alleles do not complement the deletion of the *MAD2* gene in *S. cerevisiae*.** Strains with the indicated genotypes were grown to log phase, arrested in G1 by α factor, and released in fresh medium containing nocodazole. At the indicated times, cell samples were withdrawn for FACS analysis of DNA contents (A) and to score the percentage of budded and rebudded cells as well as the percentage of sister chromatid separation (B). wt, wild type.

interaction of the O- and C-Mad2 conformers (De Antoni et al., 2005a,b). It is possible that the inability of Mad2^{RA} and Mad2^{QA} to support the SAC in *S. cerevisiae* results from the impairment of an equivalent O-Mad2–C-Mad2 interaction. However, it is unknown whether ScMad2 is endowed with the same unusual biochemical features that characterize HsMad2 and that include the ability to adopt two stable conformations and the ability of the opposite conformers to form a complex. Thus, we set out to address the important question of whether two interacting conformers of ScMad2 exist as shown previously for HsMad2 (De Antoni et al., 2005a).

For this, we first tested the ability of purified recombinant ScMad2 to bind GST fusions of the Mad2-binding motifs of ScMad1 and ScCdc20 (GST-Mad1$^{563–590}$ and GST-Cdc20$^{184–210}$) in a solid phase binding assay (Fig. 2 A). Mad2^{wt} bound effectively to GST-Cdc20 and GST-Mad1 immobilized on glutathione–Sepharose (GSH) beads (Fig. 2 A, lanes 6 and 10). As a result of the ∼40% sequence identity between HsMad2 and ScMad2 and because the Mad2-binding motifs of Mad1 and Cdc20 conform to the same consensus sequence in different species (Luo et al., 2002; Sironi et al., 2002), we assume that ScMad2 adopts a C-Mad2 conformation when bound to ScMad1 and ScCdc20 similar to that adopted by HsMad2 when bound to its human partners.

The deletion of 10 residues from the C terminus of HsMad2 (HsMad2^{ΔC}) affects the structural stability of the C-Mad2 conformer while leaving the stability of O-Mad2 untouched, creating a constitutively open form of Mad2 (Sironi et al., 2001, 2002; De Antoni et al., 2005a). Because the ability to reach the C-Mad2 conformation is critically required to bind Mad1 and Cdc20, Mad2^{ΔC} is inapt to bind Mad1 or Cdc20 even if the residues within the deletion are not in direct contact with Mad1 or Cdc20 (Luo et al., 2000; Sironi et al., 2001, 2002; De Antoni et al., 2005a).

We created an equivalent mutant of ScMad2 (ScMad2^{ΔC}) by deleting six residues from its C terminus (the C-terminal tail of ScMad2 is four residues shorter relative to HsMad2). Unlike ScMad2^{wt}, pure recombinant ScMad2^{ΔC} was unable to bind GST-Mad1$^{563–590}$ or GST-Cdc20$^{184–210}$ (Fig. 2 A, lanes 7 and 11). Essentially identical results were obtained in solution using isothermal titration calorimetry (Table S1, available at http://www.jcb.org/cgi/content/full/jcb.200602109/DC1). Thus, ScMad2^{ΔC} is a constitutively open form of Mad2 that is unable to bind Mad1 or Cdc20 and is similar in all of these respects to HsMad2^{ΔC} (Luo et al., 2000; Sironi et al., 2001; De Antoni et al., 2005a).

We next tested whether the O- and C-Mad2 conformers of ScMad2 are capable of forming a complex like their human counterparts. First, we created C-Mad2 on solid phase by allowing ScMad2^{wt} to bind GST-Mad1$^{563–590}$ and GST-Cdc20$^{184–210}$ as in the experiments shown in Fig. 2 A (lanes 6 and 10). This time, however, after washing out the excess of unbound Mad2^{wt}, we added Mad2^{ΔC} (i.e., O-Mad2) to see whether it could be retained on solid phase via an interaction with the previously bound C-Mad2^{wt}. Indeed, ScMad2^{ΔC} was found on solid phase in a complex with GST-Mad1$^{563–590}$–C-Mad2 and GST-Cdc20$^{184–210}$–C-Mad2 (Fig. 2 A, lanes 8 and 12). This confirms the existence of an interaction of O- and C-Mad2 as described previously for HsMad2 (De Antoni et al., 2005a,b).

To test whether mutating Arg126 and Gln127 affects the interaction between O- and C-Mad2, we repeated this experiment with ScMad2^{RQEA} after its expression in bacteria and purification to homogeneity. Like Mad2^{wt}, Mad2^{RQEA} bound effectively to GST-Mad1$^{563–590}$ and GST-Cdc20$^{184–210}$ (Fig. 2 B, lanes 6 and 10), indicating that this mutant can adopt the C-Mad2 conformation like Mad2^{wt}. Indeed, Mad2^{wt} and Mad2^{RQEA} bound Mad1 and Cdc20 synthetic peptides with essentially identical affinities in isothermal titration calorimetry measurements (Table S1).

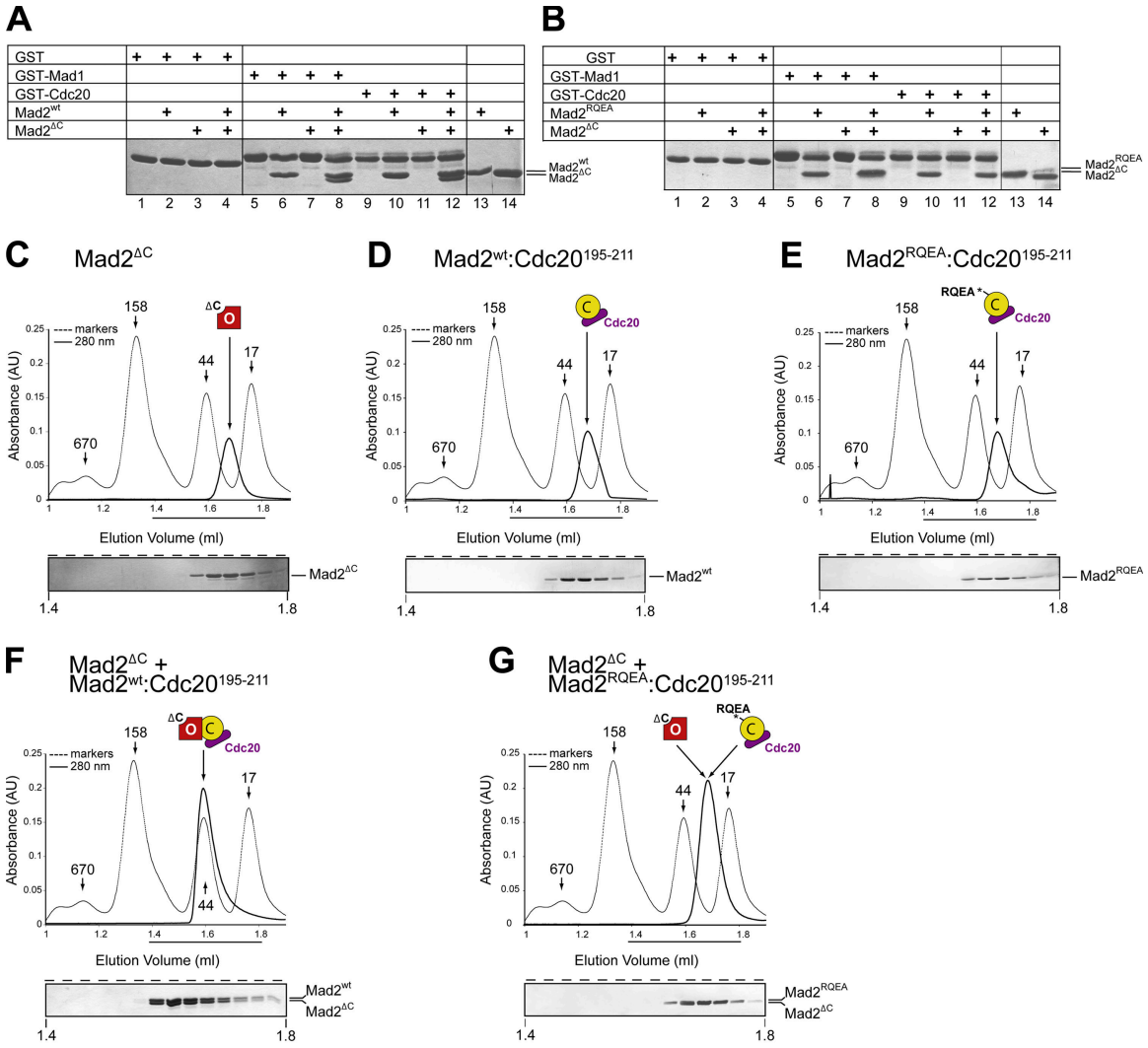

Figure 2. **The O and C conformers of ScMad2^{wt} form a complex that requires Arg126 and Gln127.** (A) GST (lanes 1–4), GST-Mad1$^{563–590}$ (lanes 5–8), and GST-Cdc20$^{184–210}$ (lanes 9–12) were immobilized on GSH beads at ~1.0 μM and incubated with ~5 μM Mad2^{wt} or Mad2$^{\Delta C}$ (lanes 13 and 14) for 1 h. GSH beads were collected by centrifugation, washed, and bound proteins were analyzed by SDS-PAGE. For samples in lanes 8 and 12, beads were incubated with ~5 μM Mad2^{wt}, washed, incubated with the same concentration of Mad2$^{\Delta C}$ for an additional hour, and analyzed by SDS-PAGE. (B) The experiment was performed as in A but with Mad2^{RQEA} and Mad2$^{\Delta C}$. Although Mad2^{RQEA} binds GST-Mad1 and Cdc20 as well as Mad2^{wt}, it is unable to bind Mad2$^{\Delta C}$ (lanes 8 and 12). (C) 50 μl of a 20-μM solution of Mad2$^{\Delta C}$ was analyzed by SEC on a Superdex-200 PC 3.2/30 column and found to elute as a monomer. The content of 14 30-μl consecutive fractions eluting between 1.4 and 1.82 ml was analyzed by SDS-PAGE and was Coomassie stained. (D) To generate C-Mad2^{wt}, 200 μM Cdc20$^{195–211}$ synthetic peptide was incubated with 20 μM Mad2^{wt} for 1 h. The sample was analyzed by SEC as in C. (E) As in D but with Mad2^{RQEA} and the Cdc20$^{195–211}$ peptide. (F) C-Mad2^{wt}–Cdc20$^{195–211}$ was mixed with Mad2$^{\Delta C}$ for 1 h before separation by SEC. Dimerization of O and C conformers was revealed by a shift in elution volume relative to O- and C-Mad2. (G) The same experiment with C-Mad2^{RQEA}–Cdc20$^{195–211}$ rather than with Mad2^{wt} shows that this double point mutant protein is unable to bind O-Mad2. AU, arbitrary unit.

Next, we incubated Mad2^{RQEA} with GST-Mad1$^{563–590}$ or GST-Cdc20$^{184–210}$ to create the closed conformer, washed away the excess of unbound Mad2^{RQEA}, and added Mad2$^{\Delta C}$ (O-Mad2). This time, we failed to observe any retention of ScMad2$^{\Delta C}$ on solid phase (Fig. 2 B, lanes 8 and 12). Given our previous analyses of the effects of mutating Arg133 and Gln134 in HsMad2 (De Antoni et al., 2005a), the conservation of these residues in ScMad2, and the identity of results with ScMad2 and HsMad2, we conclude that Arg126 and Gln127 map to the O-Mad2–binding surface of C-Mad2 and that their concomitant mutation into glutamate and alanine, respectively, prevents this interaction.

The interaction between O- and C-Mad2 was verified in solution using purified proteins (Fig. 2, C–G). Both ScMad2$^{\Delta C}$ (O-Mad2) and the complexes of Mad2^{wt} or Mad2^{RQEA} with the high affinity Cdc20$^{195–211}$ synthetic peptide (C-Mad2) eluted as apparent monomers from a Superdex-200 size-exclusion chromatography (SEC) column (Fig. 2, C–E), indicating that both O- and C-Mad2 are monomeric (although the C-Mad2 species forms dimers with the Cdc20 peptide, this is only a 17-residue segment that does not significantly change the Stokes' radius of Mad2). When combined stoichiometrically at 25°C for 60 min, ScMad2$^{\Delta C}$ and the Mad2^{wt}–Cdc20$^{195–211}$ complex formed an O–C complex that eluted with a Stokes' radius larger than that of the individual species and compatible with the molecular mass expected for an ScMad2 dimer (~48 kD, as the molecular mass of the monomeric protein is ~24 kD; Fig. 2 F).

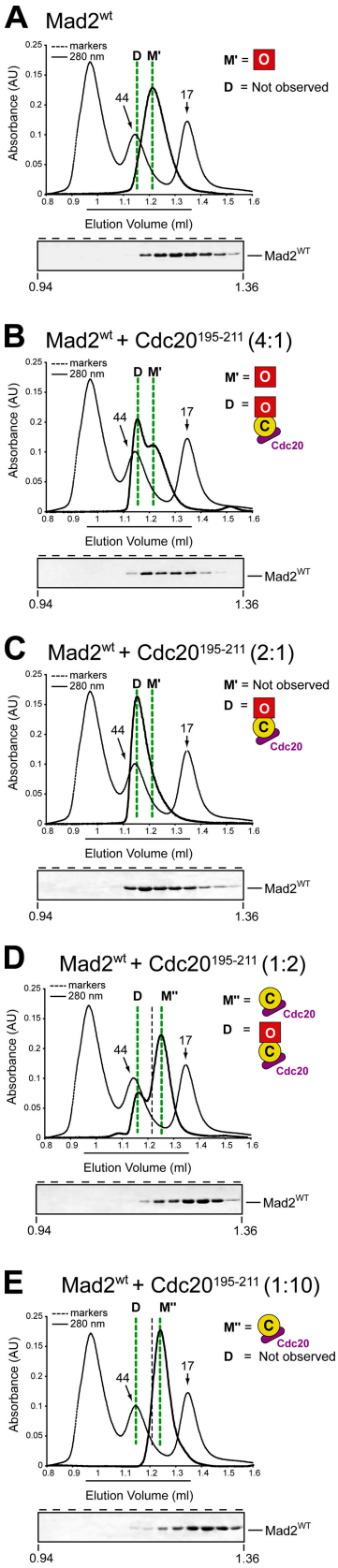

Figure 3. **Monomers and dimers of ScMad2^{wt}.** Different Mad2 species (at a concentration of 20 µM) were analyzed using a Superdex-75 PC 3.2/30 SEC column. For each panel, 14 30-µl fractions between 0.94 and 1.36 ml were analyzed by SDS-PAGE. For each panel, the elution volumes of C-Mad2–O-Mad2 dimers (D) and the O-Mad2 monomer (M′) or C-Mad2 monomer (M′′) are marked. In D and E, the black dotted lines mark the elution volume of M′ (O-Mad2), which is shifted relative to M′′. (A) Pure ScMad2 eluted as a monomer. (B) Upon the addition of Cdc20$^{195–211}$ at 1/4 of the Mad2 concentration, ∼50% of Mad2 is shifted into a dimer peak. (C) Cdc20$^{195–211}$ at 1/2 of the Mad2 concentration causes most Mad2 to shift into a dimer peak. (D) Upon the addition of superstoichiometric Cdc20, a C-Mad2 monomer accumulates. (E) The process of the creation of C-Mad2–Cdc20 is complete. AU, arbitrary unit.

Fractions corresponding to this peak contained apparently stoichiometric amounts of each component. When ScMad2$^{\Delta C}$ was combined with Mad2^{RQEA}–Cdc20$^{195–211}$ and the result of the incubation was analyzed by SEC, no equivalent shift in the elution profile was observed (Fig. 2 F). Although ScMad2$^{\Delta C}$ coeluted with Mad2^{RQEA}–Cdc20$^{195–211}$, the comparison of the peak of elution with those of the individual proteins displayed in Fig. 2 (C and E) clarifies that this was simply caused by the overlap of two distinct peaks with essentially identical elution volumes. These results confirm that the RQEA mutation affects the interaction of C- with O-Mad2.

We also investigated the state of the oligomerization of ScMad2^{wt}. Pure ScMad2^{wt} eluted from a Superdex-75 SEC column as a monomer (Fig. 3 A). To assess whether this monomer is O-Mad2, as expected for Mad2 in the absence of Mad1 or Cdc20, we examined the effects of adding increasing concentrations of the Cdc20$^{195–211}$ synthetic peptide on the SEC profile of ScMad2^{wt}. At a 4:1 Mad2/Cdc20$^{195–211}$ ratio, a dimeric species roughly engaging 50% of total Mad2 appeared (Fig. 3 B). This can be easily explained if we assume that Cdc20$^{195–211}$ transformed ∼1/4 of O-Mad2 in C-Mad2 and that this bound to an equimolar amount of O-Mad2, leaving half of the original O-Mad2 in the monomer peak. (As mentioned in the previous paragraph, the O–C dimer is actually a trimer if we consider Cdc20$^{195–211}$, but the latter does not contribute significantly to the elution profile of the O–C-Mad2 dimer.) Consistent with this hypothesis, at a 2:1 Mad2/Cdc20$^{195–211}$ ratio, most Mad2 eluted as a dimer (Fig. 3 C). When the Mad2/Cdc20$^{195–211}$ ratio was decreased to cause the conversion of more O-Mad2 to C-Mad2–Cdc20$^{195–211}$, the Mad2 dimer progressively disappeared, whereas a monomer peak corresponding to C-Mad2–Cdc20$^{195–211}$ accumulated (Fig. 3, D and E). (Again, this is technically a dimer whose elution is not significantly influenced by Cdc20$^{195–211}$). The elution volume of the C-Mad2 monomer was slightly but consistently retarded relative to that of the O-Mad2 monomer.

Altogether, the experiments in Figs. 2 and 3 strongly suggest that the O and C conformers of ScMad2 form a dimeric complex like the one previously described for the equivalent conformers of HsMad2 (De Antoni et al., 2005a,b). The similarity with HsMad2 extends to the fact that neither conformer forms dimers without the other conformer, contrary to the proposition that C-Mad2 forms dimers (Luo et al., 2004). Furthermore, our data indicate that the interface containing Arg126 and Q127 of C-Mad2 is important for binding O-Mad2. In Fig. 4, we show that the converse is also true: namely, that a similar (but most likely not identical) interface in O-Mad2 is important for binding C-Mad2.

Binding of O-Mad2 to the Mad1–C-Mad2 complex

Mad1 and Cdc20 bind the same Mad2 pocket and generate structurally similar C-Mad2 conformers. We have proposed that kinetochore recruitment of Mad2 requires a tight Mad1–Mad2 complex at the kinetochore whose C-Mad2 component offers the critical binding surface for cytosolic O-Mad2 (Sironi et al., 2002; De Antoni et al., 2005a). To test whether this is also the case for ScMad2, we created a recombinant ScMad1–ScMad2 complex and purified it to homogeneity (Fig. 4 A). This complex lacks the kinetochore-binding domain of Mad1 (located in the N-terminal half of Mad1) but contains coiled-coil segments that mediate the dimerization of Mad1 and two Mad2-binding domains, one per Mad1 chain, that are required for high affinity binding of Mad2. The resulting complex contains a very stable tetrameric core, as shown previously for an equivalent human complex (Sironi et al., 2001, 2002). Although we have not analyzed the stability of the ScMad1$^{529–750}$–ScMad2 complex in detail, we failed to observe any changes in the relative stoichiometry of its components during purification, suggesting it is very stable.

To test the ability of purified O-Mad2 to bind C-Mad2 in the Mad1–Mad2 complex, we covalently attached the AlexaFluor488 fluorophore to ScMad2^{wt}, ScMad2$^{\Delta C}$, or ScMad2^{RQEA}. We analyzed the resulting labeled proteins by SEC using a Superdex-200 column (Fig. 4, B–D) after the elution of AlexaFluor488-labeled Mad2 at 280 and 495 nm (Fig. 4, B–D; black and green traces, respectively). Excitation of the AlexaFluor fluorophore at 300 nm using a UV trans-illuminator provided a useful means of detecting the labeled protein in elution fractions after SDS-PAGE separation. The same gels were also stained with Coomassie (Fig. 4, B–D; top and bottom gel sections). This revealed that all three proteins eluted from the SEC column apparently as monomers.

We then mixed stoichiometric amounts of the fluorescent Mad2 species to the Mad1–Mad2 complex (at concentrations of ~20 μM of monovalent Mad2 and 10 μM of divalent Mad1–Mad2 core complex) and, after a 1-h incubation, we analyzed the products by SEC. AlexaFluor-labeled ScMad2^{wt} and ScMad2$^{\Delta C}$ bound Mad1–Mad2 with high affinity, as evidenced by the essentially complete shift of the AlexaFluor fluorophore to fractions containing the Mad1–Mad2 core complex (Fig. 4, E and F). On the other hand, AlexaFluor-ScMad2^{RQEA} was unable to bind the Mad1–Mad2 core complex (Fig. 4 G). Addition of the Cdc20$^{195–211}$ synthetic peptide (at 200 μM) to "external" AlexaFluor–O-Mad2^{wt} prebound to the Mad1–Mad2 core complex resulted in dissociation of the AlexaFluor-labeled species in a low molecular weight complex, presumably in a complex with the Cdc20 peptide (Fig. 4 H). However, when the complex of O-Mad2$^{\Delta C}$ with Mad1–Mad2 was tested with Cdc20$^{195–211}$, neither Mad2$^{\Delta C}$ nor C-Mad2 that bound to Mad1 was released in a complex with Cdc20$^{195–211}$ (Fig. 4 I). This is consistent with the inability of Mad2$^{\Delta C}$ to bind Cdc20 and shows that the Mad1–Mad2 complex is stable and is not disrupted by Cdc20. Consistently, C-Mad2 in the Mad1–Mad2 complex did not dissociate from Mad1 if Cdc20$^{195–211}$ was added in the absence of external O-Mad2 (unpublished data).

Overall, these results are indistinguishable from those previously described for HsMad2 and its interaction with Mad1 and Cdc20 (De Antoni et al., 2005a) and indicate that the O-Mad2 conformer of ScMad2 binds the C-Mad2 conformer in the Mad1–Mad2 complex. Because Mad2$^{\Delta C}$ is unable to bind Mad1, whereas Mad2^{RQEA} is a normal Mad1 ligand, we conclude that Mad1 binding is not required for the binding reaction analyzed in Fig. 4. Rather, the interaction involves a surface predominantly or exclusively based on O- and C-Mad2. The experiments reported in Fig. 4 show that O-Mad2^{RQEA} is unable to bind the wild-type C-Mad2 protein in the Mad1–Mad2 complex. Conversely, in Fig. 2, these mutations were shown to affect the binding to a functional O-Mad2 (ScMad2$^{\Delta C}$, whose deficiency consists uniquely in being unable to turn into C-Mad2). Thus, the surface containing Arg126 and Gln127 is involved in Mad2 dimerization both on the O and C conformers.

Conformational analysis of O- and C-Mad2

Previous structural investigations demonstrated that human Mad2$^{\Delta C}$ has the O-Mad2 conformation, that Mad2^{wt} and Mad2^{R133A} bound to Cdc20 or Mad1 are folded as C-Mad2, and that the two human conformers O- and C-Mad2 bind each other (Luo et al., 2000, 2002, 2004; Sironi et al., 2002; De Antoni et al., 2005a,b). For instance, human O-Mad2$^{\Delta C}$ binds human Mad1–C-Mad2 (Fig. 5 A), which is a completely analogous reaction to that involving yeast proteins in Fig. 4 F. So far, we assumed that ScMad2 adopts O- and C-Mad2 conformations whose encounter results in their dimerization as for HsMad2. Although a direct structural investigation of the conformational states of ScMad2 goes beyond the purpose of this study, we wished to provide stronger evidence that ScMad2 adopts O- and C-Mad2 conformations like HsMad2. If ScMad2$^{\Delta C}$ has the O-Mad2 conformation previously characterized for HsMad2$^{\Delta C}$, it might be expected to bind human C-Mad2. To test this, we mixed stoichiometric amounts of human Mad1–C-Mad2 complex (Sironi et al., 2002) with AlexaFluor-ScMad2$^{\Delta C}$ and analyzed the resulting species by SEC on a Superdex-200 column (Fig. 5 B). Confirming our expectation that ScMad2$^{\Delta C}$ has the same O-Mad2 conformation that was previously demonstrated for HsMad2$^{\Delta C}$ (Luo et al., 2000), AlexaFluor-ScMad2$^{\Delta C}$ co-eluted with the human Mad1–C-Mad2 complex. Binding was specific because AlexaFluor-ScMad2^{wt} that preincubated with the ScCdc20$^{195–211}$ synthetic peptide to create C-Mad2 failed to bind the human Mad1–Mad2 complex (Fig. 5 C).

Conversely, if Mad1-bound ScMad2 has the same C-Mad2 conformation previously observed in the structure of the human Mad1–C-Mad2 complex (Sironi et al., 2002), it might be expected to bind human Mad2$^{\Delta C}$, which has been shown to fold as O-Mad2 (Luo et al., 2000). Indeed, AlexaFluor-HsMad2$^{\Delta C}$ bound tightly to the *S. cerevisiae* Mad1–Mad2 complex (Fig. 5 D), strongly suggesting that the conformation of ScMad2 bound to ScMad1 is C-Mad2. Preincubation of HsMad2^{wt} with a synthetic peptide encompassing the Mad2-binding site of HsCdc20 (Cdc20$^{111–138}$) to create human C- Mad2 prevented its binding to the *S. cerevisiae* Mad1–Mad2 complex (Fig. 5 E). These experiments indicate that the interface mediating the interaction of O- with C-Mad2 is strongly conserved in evolution

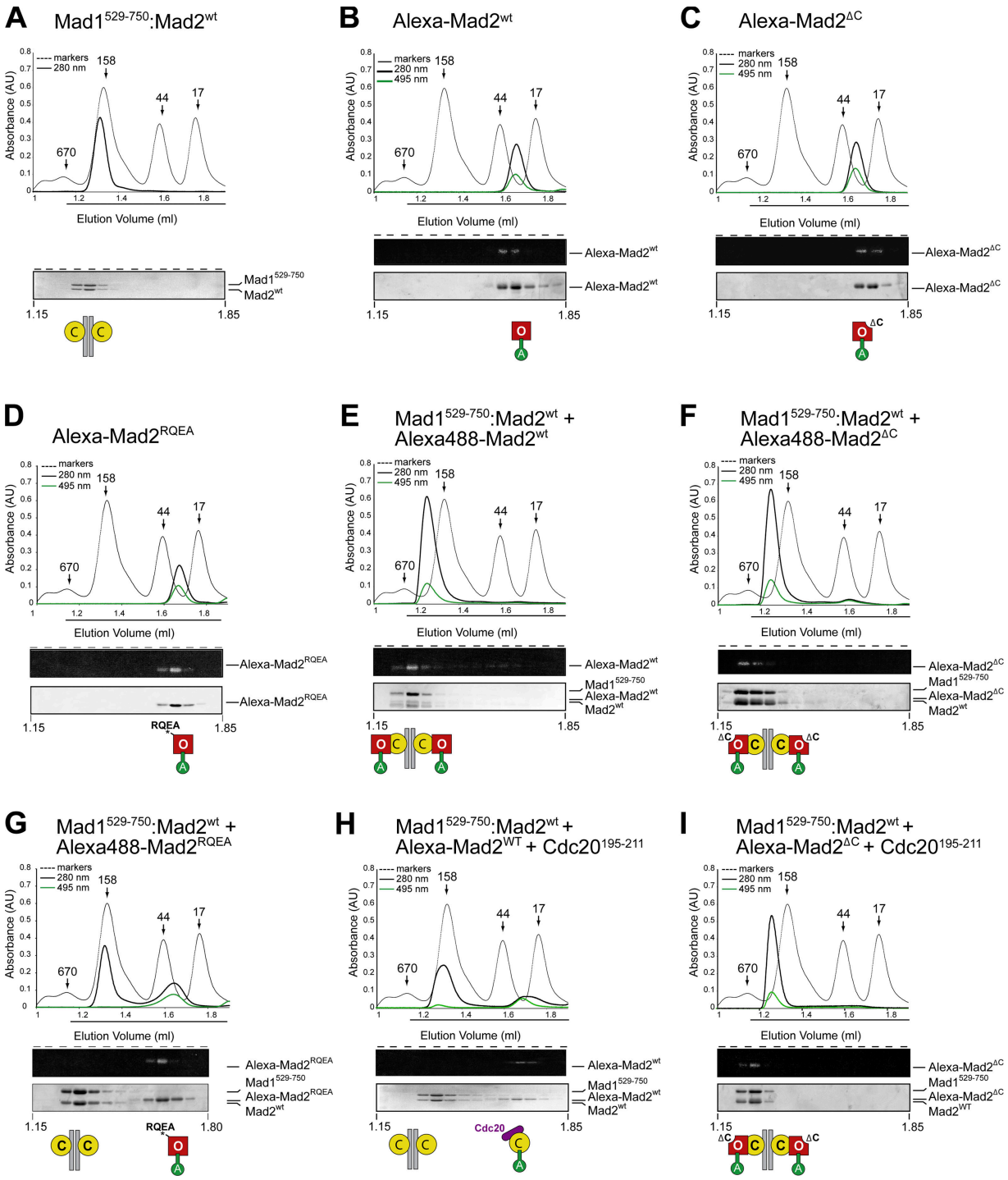

Figure 4. **O-Mad2 binds the Mad1–Mad2 core complex.** (A) Mad1–Mad2 forms a stable tetrameric assembly, the Mad1–Mad2 core complex (Sironi et al., 2002). A recombinant yeast complex containing the C-terminal region of Mad1 (residues 529–750 lacking the N-terminal kinetochore-binding domain of Mad1) was coexpressed in bacteria with Mad2^{wt}, and the resulting complex was purified to homogeneity (see Materials and methods). 50 μl Mad1–Mad2 complex (10 μM) was analyzed by SEC on a Superdex-200 PC 3.2/30 column. Fractions between 1.15 and 1.85 ml were analyzed by SDS-PAGE. (B) SEC profile of Mad2^{wt} covalently labeled with AlexaFluor488. The content of the elution fractions was analyzed after SDS-PAGE on a UV trans-illuminator (top) and by Coomassie staining (bottom). (C and D) AlexaFluor488-Mad2$^{\Delta C}$ (C) and AlexaFluor488-Mad2^{RQEA} (D) was analyzed as in B. (E) Mad2^{wt} (O-Mad2) was incubated stoichiometrically with Mad1$^{529–750}$–Mad2^{wt}, and the resulting sample was analyzed by SEC. Most of the AlexaFluor488 signal associated with Mad2^{wt} was incorporated in a high molecular weight complex, indicating binding to Mad1–Mad2. (F) The same experiment was repeated using AlexaFluor488-Mad2$^{\Delta C}$. Also in this case, the AlexaFluor signal was shifted to a high molecular weight complex with Mad1–Mad2. (G) AlexaFluor488-Mad2^{RQEA} fails to bind Mad1–Mad2, indicating that Arg126 and Gln127 are part of the binding interface. (H) Mad2^{wt} was incubated stoichiometrically with Mad1$^{529–750}$–Mad2^{wt} in the presence of Cdc20$^{195–211}$. The AlexaFluor488 signal associated with Mad2^{wt} is released from the Mad1–Mad2 complex. (I) As in H but with AlexaFluor488-Mad2$^{\Delta C}$, which does not bind Cdc20 and is not released from Mad1–Mad2. AU, arbitrary unit.

(as already exemplified by the conservation of R126 and Q127), underscoring the biological importance of Mad2 dimerization in checkpoint function.

Mad2$^{\Delta C}$ abrogates the checkpoint

The results of our biochemical characterization of ScMad2 are consistent with the Mad2 template model (De Antoni et al., 2005a,b). The latter depicts C-Mad2 stably bound to Mad1 (rather than Mad1 itself) as a trigger that is required for Mad2 to bind Cdc20 in living cells. In this view, the absolute requirements for Mad1 in activating Mad2 for Cdc20 binding are limited to its function in localizing a pool of C-Mad2 to the kinetochore. This form of C-Mad2 recruits O-Mad2 from the cytosol to assist in its transformation into C-Mad2 bound to Cdc20. To provide more evidence in favor of this model, we asked whether interfering with the O–C-Mad2 interaction weakens the SAC response. Because O-Mad2$^{\Delta C}$ binds C-Mad2 but is unable to be passed onto Cdc20 (Fig. 4), this mutant is expected to compete with the binding of O-Mad2^{wt} to C-Mad2, and we asked whether its expression perturbed the SAC response in *S. cerevisiae*. First, we determined that ScMad2$^{\Delta C}$ expressed from the endogenous *MAD2* promoter is unable to sustain the checkpoint in a *mad2Δ* strain (Fig. S1, A and B; available at http://www.jcb.org/cgi/content/full/jcb.200602109/DC1), which is consistent with a previous study (Chen et al., 1999) and with our own observation that ScMad2$^{\Delta C}$ is unable to bind Mad1 or Cdc20.

To test our hypothesis, we expressed ScMad2$^{\Delta C}$ from the *GAL1* promoter and tested checkpoint function after the release of wild-type cells from a G1 arrest in nocodazole (Fig. 6). As expected, cells overexpressing ScMad2$^{\Delta C}$ but not those overexpressing full-length ScMad2 in a wild-type background lost sister chromatid cohesion and rebudded and re-replicated their chromosomes, which is indicative of a checkpoint defect. Thus, ScMad2$^{\Delta C}$ has a dominant-negative effect on the SAC analogous to that observed in vertebrate cells (Chen et al., 1999;

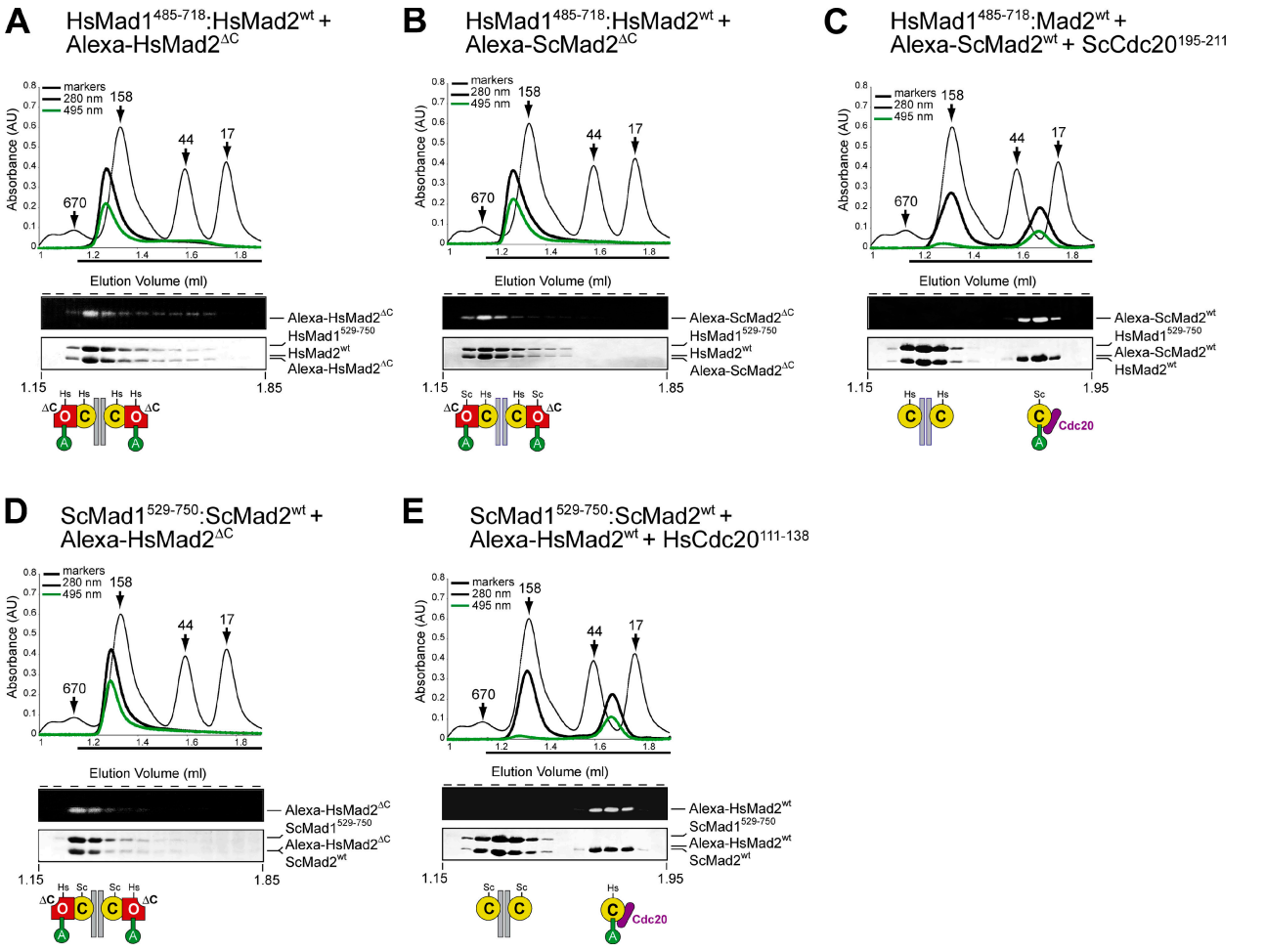

Figure 5. **The O–C interaction of Mad2 is conserved in evolution.** (A) Human O-Mad2 binds the Mad1–C-Mad2 complex. 50 µl of human Mad1–Mad2 complex (10 µM of divalent complex) was combined stoichiometrically with 20 µM of human AlexaFluor488-Mad2$^{\Delta C}$ and analyzed by SEC on a Superdex-200 PC 3.2/30 column. Fractions between 1.15 and 1.85 ml were analyzed by SDS-PAGE. Human Mad1–Mad2 and Mad2 were expressed and purified as described previously (De Antoni et al., 2005a). (B) AlexaFluor488-Mad2$^{\Delta C}$ from *S. cerevisiae* was incubated with human Mad1–Mad2 and analyzed as in A. (C) AlexaFluor488-ScMad2^{wt} was incubated with ScCdc20$^{195–212}$. This yeast C-Mad2–Cdc20 complex did not bind human Mad1–Mad2. (D) AlexaFluor488-HsMad2$^{\Delta C}$ was incubated stoichiometrically with yeast Mad1–Mad2 and analyzed as in A. (E) AlexaFluor488-HsMad2^{wt} was incubated with a synthetic peptide encompassing the Mad2-binding segment of HsCdc20 (Cdc20$^{111–138}$). This human C-Mad2–Cdc20 complex did not bind yeast Mad1–Mad2. AU, arbitrary unit.

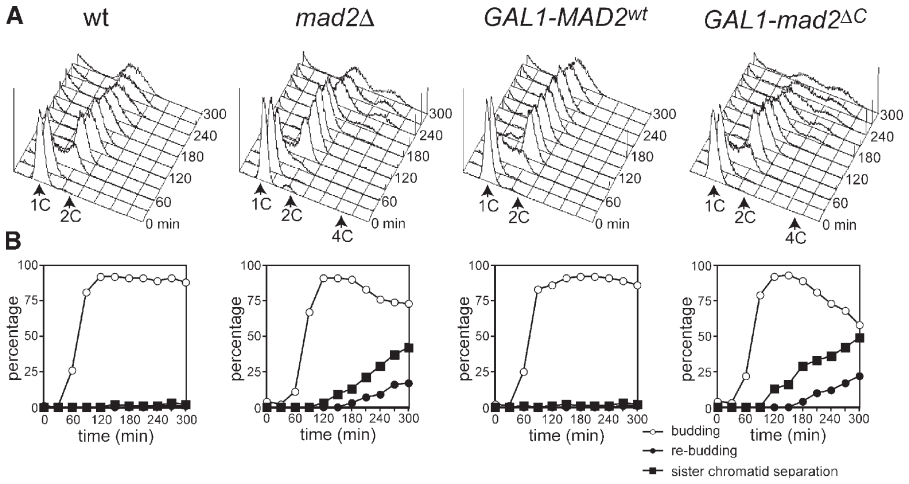

Figure 6. **Mad2$^{\Delta C}$ has a dominant-negative effect on the checkpoint.** Strains with the indicated genotypes were grown to log phase in YEPR medium, arrested in G1 by α factor, and released into YEPRG medium containing nocodazole. 1% galactose was added to the cultures half an hour before the release to induce the *GAL1* promoter. At the indicated times, cell samples were withdrawn for FACS analysis of DNA contents (A) and to score the percentage of budded and rebudded cells as well as the percentage of sister chromatid separation (B).

Canman et al., 2002; De Antoni et al., 2005a), which is in agreement with our hypothesis that this mutant interferes with the interaction of Mad2^{wt} with Cdc20. Although we have been thus far unable to coimmunoprecipitate the complex between ScMad2$^{\Delta C}$ and the Mad1–Mad2 complex, we show that ScMad2$^{\Delta C}$ overexpressed from the *GAL1* promoter in a *mad2Δ* strain was unable to bind Mad1 (Fig. S1 C).

Mad2^{R126A} and Mad2^{Q127A} bind Mad1 normally but fail to bind Cdc20 in vivo

As shown in Fig. 2 and in Table S1, Mad2^{wt} and Mad2^{RQEA} bind Mad1 and Cdc20 effectively in vitro (the single mutants Mad2^{RA} and Mad2^{QA} bind equally well; unpublished data). However, the reintroduction of *MAD2^{wt}* at the endogenous *LEU2* locus of a *mad2Δ* strain restored the SAC, whereas the expression of *mad2^{RA}* and *mad2^{QA}* failed to do so (Fig. 1). Because our model proposes that the interaction of the Mad2 conformers is essential to activate Mad2 for Cdc20 binding, Mad2 mutants that are unable to sustain this interaction should be unable to reach Cdc20 in living cells. We decided to assess the amounts of Mad1 and Cdc20 that bound to Mad2^{wt}, Mad2^{RA}, and Mad2^{QA} expressed in a *mad2Δ* background. The association of Mad1 with Mad2 is not regulated during the cell cycle (Chen et al., 1999). To test the ability of Mad2 and its mutant variants to bind Mad1, we performed Mad1-myc18 immunoprecipitations (IPs) from cycling cells of *MAD1-myc18 MAD2* and *MAD1-myc18 mad2Δ* strains carrying the *MAD2^{wt}*, *mad2^{RA}*, and *mad2^{QA}* alleles integrated at the *LEU2* locus. Consistent with their ability to bind Mad1 in vitro, Mad2^{RA} and Mad2^{QA} were found to associate with Mad1 in vivo as efficiently as Mad2^{wt} (Fig. 7 A).

Unlike the levels of Mad1 and Mad2, which are essentially constant during the cell cycle, Cdc20 is a cell cycle–regulated protein whose destruction is required for mitotic exit (Peters, 2002). Thus, we investigated the levels of Mad2 and its mutant variants associated with Cdc20 during mitosis, when *CDC20* expression is maximal (Peters, 2002). For this, *myc18-CDC20 MAD2* cells and *myc18-CDC20 mad2Δ* cells carrying the *MAD2^{wt}*, *mad2^{RA}*, and *mad2^{QA}* alleles integrated at the *LEU2* locus were arrested in G1 with α factor and were released into the cell cycle in the presence of nocodazole, which activates the SAC, promoting the formation of the Mad2–Cdc20 complex. All three strains reentered the cell cycle normally and completed DNA replication synchronously roughly 60 min after release

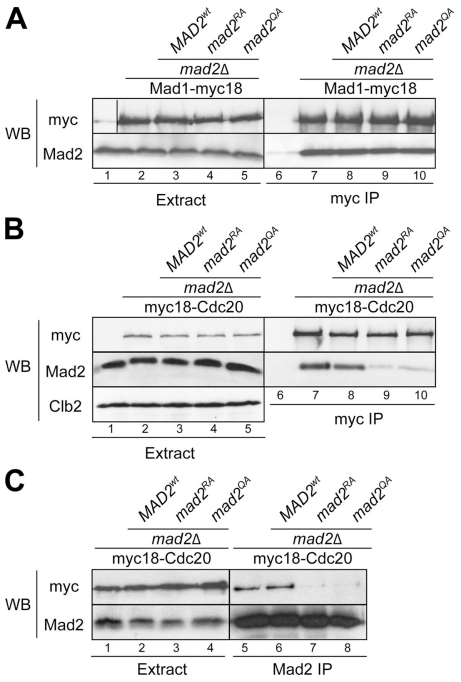

Figure 7. **Mutations in the binding interface between O- and C-Mad2 impair Cdc20 binding.** (A) Protein extracts were prepared from cycling cells of untagged wild-type (W303; lanes 1 and 6), *MAD1-myc18 MAD2* (ySP2218; lanes 2 and 7), and *MAD1-myc18 mad2Δ* strains carrying the *MAD2^{wt}* (ySP5314; lanes 3 and 8), *mad2^{RA}* (ySP5316; lanes 4 and 9), and *mad2^{QA}* (ySP5318; lanes 5 and 10) alleles integrated at the *LEU2* locus. Total extracts and anti-myc IPs were analyzed by Western blotting (WB) to detect Mad1-myc18 and Mad2. (B) Cycling cultures of untagged wild-type (W303; lanes 1 and 6), *myc18-CDC20 MAD2* (ySP1413; lanes 2 and 7), and *myc18-CDC20 mad2Δ* strains carrying, respectively, the *MAD2^{wt}* (ySP5311; lanes 3 and 8), *mad2^{RA}* (ySP5355; lanes 4 and 9), and *mad2^{QA}* (ySP5356; lanes 5 and 10) alleles integrated at the *LEU2* locus were arrested in G1 by α factor and released in the presence of nocodazole. After 80 min, cells were collected, and protein extracts were used for IPs with anti-myc antibodies. FACS analysis (not depicted) confirmed that cells were in G2/M. Total extracts and immunoprecipitates were analyzed by Western blotting to visualize myc18-Cdc20 and Mad2. (C) The same extracts as in B were used for IPs with anti-Mad2 polyclonal antibodies and analyzed by Western blotting as in B.

from the arrest. To assess the amounts of Mad2 bound to Cdc20, IPs were performed from extracts of cells harvested 80 min after release from the G1 arrest. To confirm that these cells were in mitosis regardless of their genotype, we monitored the levels of the mitotic cyclin Clb2. These were found to be identical (Fig. 7 B), showing that both checkpoint-proficient (*MAD2*^{wt}) and checkpoint-deficient (*mad2*^{RA} or *mad2*^{QA}) cells had been harvested while in mitosis. Although Mad2^{wt} expressed in *mad2Δ* cells bound normally to myc-Cdc20, the binding of Mad2^{RA} and Mad2^{QA} to myc-Cdc20 was severely impaired (Fig. 7 B). In the converse experiment, we found greatly diminished levels of myc-Cdc20 in Mad2 IPs (Fig. 7 C). Overall, these results indicate that the differences in the amount of Mad2–Cdc20 complex in cells expressing Mad2^{wt}, Mad2^{RA}, or Mad2^{QA} must be the result of the inability of the mutant proteins to support the interaction of O- with C-Mad2. We conclude that this interaction represents a critical step in the activation of Mad2 in the SAC.

Discussion

In this study, we show that two critical features of Mad2—the ability to adopt open and closed conformations and dimerization of the open and closed conformers—are both likely to be conserved in all eukaryotes. Both features appear to be required for Mad2 to bind Cdc20 and to sustain the checkpoint. We provide convincing evidence that recombinant ScMad2 folds as an O-Mad2 monomer that changes its conformation to C-Mad2 upon binding Mad1 or Cdc20. Recombinant HsMad2 forms oligomers in the absence of Mad1 or Cdc20 (Fang et al., 1998). We have reanalyzed the mechanism of oligomerization of HsMad2 and found that the Mad2 oligomers are O–C dimers created by the partial, spontaneous conversion of O-Mad2 into an "empty" C-Mad2 (i.e., devoid of Mad1 or Cdc20), which, in turn, binds the remaining O-Mad2 (De Antoni et al., 2005b). Thus, HsMad2 oligomerization in vitro (Fang et al., 1998) appears to be based on the same O–C Mad2 interaction supporting the checkpoint but in the absence of Mad2 ligands. We suspect that empty C-Mad2 is unlikely to be the active Mad2 species, as proposed recently (Luo et al., 2004). Our skepticism in regarding empty C-Mad2 as the direct binder of Cdc20 is based on the fact that the specific closed conformation of the Mad2 C-terminal tail would prevent the loading of Cdc20 onto empty C-Mad2 (Musacchio and Hardwick, 2002; Sironi et al., 2002). It seems sensible to suggest that if empty C-Mad2 ever formed in living cells, it would then need to unfold its C-terminal tail to be able to bind Cdc20. The reason why recombinant HsMad2 rearranges spontaneously to create empty C-Mad2, whereas recombinant ScMad2 does not appear to do so, is currently unclear.

Our work shows identical mechanisms of O–C oligomerization for ScMad2 and HsMad2. As for HsMad2 (De Antoni et al., 2005b), the O- and C-Mad2 conformers of ScMad2 bind each other, whereas neither of them forms oligomers on their own. These observations are inconsistent with the proposition that C-Mad2 forms C–C dimers (Luo et al., 2004). However, our results are completely consistent with an earlier study from the same authors showing that C-Mad2 created using the Mad2-binding site of Cdc20 is a monomer (Luo et al., 2002). It is interesting to observe that because O–O and C–C dimers are not observed, there is a logical requirement for the O- and C-Mad2 surfaces involved in the O–C interaction to be different. The identification of residues whose mutation into alanine prevents binding of the mutant C-Mad2 conformer to wild-type O-Mad2 while leaving unaltered the ability of the mutant O conformer to bind wild-type C-Mad2 (Mapelli et al., 2006) confirms the idea that the specificity of the O–C dimerization is caused by elements of structural asymmetry.

Conversely, Arg126 and Gln127 belong to a class of "symmetric" residues whose mutation affects binding to the opposite conformer both in the O and C state (suggesting, but not implying, that some level of symmetry at the O–C interface might also be present). This gives us an opportunity to explain our choice for using single or double point mutants of Arg126 and Gln127 (Mad2^{RA} or Mad2^{QA} vs. Mad2^{RQEA}) in different experiments. Although single point mutants Mad2^{RA} and Mad2^{QA} display significant residual binding to a wild-type version of the opposite conformer, the double mutant Mad2^{RQEA} is significantly more penetrant and devoid of any significant residual binding activity toward the opposite conformer of Mad2^{wt} (De Antoni et al., 2005a,b). Thus, we will use Mad2^{RQEA} if we want to test the interaction of a mutant Mad2 conformer to the opposite conformation of Mad2^{wt}. On the other hand, the single point mutants Mad2^{RA} or Mad2^{QA} will be sufficient to disrupt binding if both binding interfaces are mutated. Accordingly, *mad2*^{RA} and *mad2*^{QA} alleles that are reintroduced in a *mad2Δ* strain are unable to reconstitute the SAC. In vitro, the level of disruption of the O-Mad2–C-Mad2 interaction observed in this case is roughly similar to that observed when testing the double point mutant RQEA against a wild-type surface (De Antoni et al., 2005b).

Fig. 8 provides a schematic account of the Mad2 template model. A stable Mad1–C-Mad2 complex recruits O-Mad2 from the cytosol via the O–C-Mad2 interaction, favoring its transformation into C-Mad2 bound to Cdc20. Strong in vivo evidence for the Mad2 template model comes from FRAP experiments revealing the presence of two distinct and quantitatively equivalent kinetochore pools of Mad2 with fast and slow turnover (Shah et al., 2004; Vink et al., 2006). In the molecular description of the Mad2 template model, the stable and mobile pools of Mad2 coincide with Mad1-bound C-Mad2 and C-Mad2–bound O-Mad2, respectively. Formal proof that these two pools account for the FRAP rates observed in vivo needs to be provided.

Because our data show that the Mad2–Cdc20 interaction in yeast requires O-Mad2–C-Mad2 binding, it is puzzling that Mad2 and Cdc20 bind spontaneously in vitro. A possible explanation for this apparent discrepancy is that the noncatalyzed rate of formation of the Mad2–Cdc20 complex is too slow to allow the accumulation of Mad2–Cdc20 that is required to sustain the SAC (Fig. 8). We speculate that the mechanistic significance of the interaction of O-Mad2 with Mad1-bound C-Mad2 is that the latter acts as a catalyst for the otherwise slow transformation of O-Mad2 into Cdc20-bound C-Mad2. A large energy barrier (and correspondingly slow kinetics) is expected for the conformational change required to turn O-Mad2 into C-Mad2, which implies the reorganization of an entire β sheet (Luo et al., 2002,

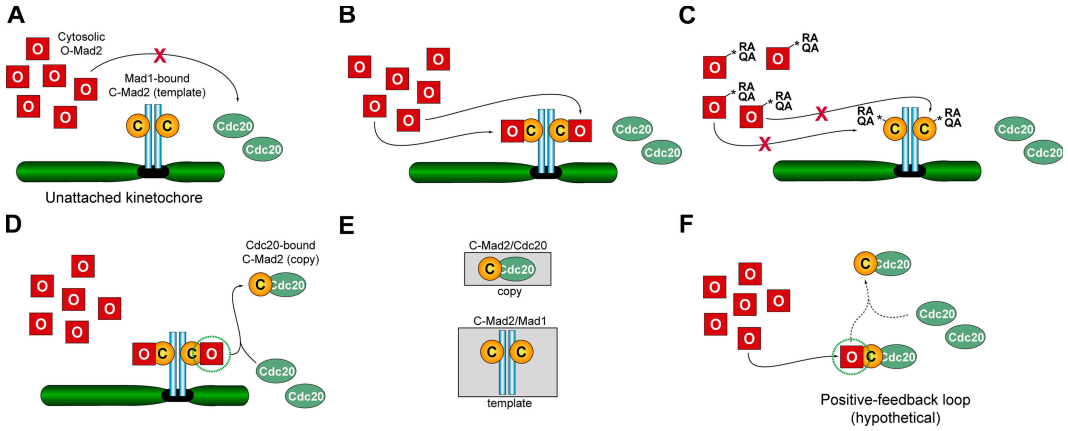

Figure 8. **Implications of the Mad2 template model.** (A) There are two pools of Mad2: a cytosolic O-Mad2 pool and a C-Mad2 pool bound to Mad1. The latter is a template required to create C-Mad2 bound to Cdc20, the "copy." In the absence of Mad1–Mad2, the Mad2–Cdc20 complex does not form efficiently. We speculate that the binding reaction, which implies a big conformational change for Mad2, is slow. (B) O-Mad2 is recruited from the cytosolic to Mad1–Mad2 at the kinetochore. Within the core complex, C-Mad2 is responsible for the interaction with O-Mad2. (C) Recruitment to the Mad1–Mad2 complex is impaired if Mad2 contains mutations such as RA and QA that affect its ability to bind O-Mad2. Under these conditions, the checkpoint cannot be activated. (D) The O-Mad2 molecule bound to C-Mad2 binds Cdc20 to create a new C-Mad2 conformer. The green circle enclosing O-Mad2 signifies that this monomer, not the C-Mad2 monomer bound to Mad1, is transferred to Cdc20. The representation of this monomer as O-Mad2 is possibly a simplification. Because we presume that prior binding of O-Mad2 to C-Mad2 accelerates binding to Cdc20 relative to cytosolic O-Mad2, this monomer might be characterized by a partially unfolded conformation of the C-terminal tail of Mad2, representing a transition state from the open to the closed conformation. (E) The C-Mad2–Cdc20 complex is a copy of the C-Mad2–Mad1 complex (the template). The decisive difference between these complexes is likely that Mad1–Mad2 is very stable, whereas Cdc20–Mad2 exists transiently and its concentrations can be reversed. (F) The Mad2 template hypothesis postulates that C-Mad2–Cdc20 acts in the cytosol like C-Mad2–Mad1 at the kinetochore. The reaction is similar to that shown in B. In comparison with C, it is easy to see that the RA and QA Mad2 mutants will also be unable to promote this step. The hypothetical reaction shown in this panel has the character of a positive feedback loop.

2004; Sironi et al., 2002). C-Mad2 may trigger the reorganization of the C-terminal tail of O-Mad2, creating a structural intermediate for its conversion into C-Mad2. The enrichment of Cdc20 at kinetochores would also favor its capture in a C-Mad2–Cdc20 complex. This reaction may also be negatively regulated. A negative regulator of the SAC such as p31^{comet} (Habu et al., 2002; Xia et al., 2004), which binds exclusively to C-Mad2 and, therefore, is likely to act as a competitor of O-Mad2, might be expected to decrease the levels of C-Mad2 available to bind O-Mad2. However, a functional homologue of this protein has not yet been identified in *S. cerevisiae*, so the generality of this hypothesis remains unclear.

The fact that a mutational impairment of the O-Mad2–C-Mad2 interaction abrogates the SAC acts in support of the Mad2 template model. Our experiments are unable to distinguish whether the C-Mad2–O-Mad2 interaction specifically requires Mad1-bound C-Mad2. More specifically, it is possible that this interaction also involves Cdc20-bound C-Mad2 in a positive feedback loop (Fig. 8 F) as we have suggested previously (De Antoni et al., 2005a,b). Thus, it will now be essential to dissect the specific functions of the C-Mad2 pools bound to Mad1 and Cdc20.

Materials and methods

Yeast strains, media, and reagents

Standard genetic techniques were used to manipulate yeast strains (Sherman, 2002). All yeast strains were derivatives of W303 (*ade2-1, trp1-1, leu2-3, 112, his3-11, 15, ura3,* and *ssd1*) and are listed in Table I. Cells were grown in YEP medium (1% yeast extract, 2% bactopeptone, and 50 mg/l adenine) supplemented with 2% glucose (YEPD), 2% raffinose (YEPR), or 2% raffinose and 1% galactose (YEPRG). α Factor was used at 2 μg/ml, and nocodazole was used at 15 μg/ml. All strains were normally grown at 25°C.

Plasmid construction and genetic manipulations

pGEX-*ScMAD1*$^{563–590}$ and pGEX-*ScCDC20*$^{184–210}$ contain the coding sequence of ScMad1$^{563–590}$ and Cdc20$^{184–210}$, respectively. pET43-*ScMAD2*–6His-*ScMAD1*$^{529–750}$ contains the coding sequence of *S. cerevisiae MAD2* separated from *S. cerevisiae* 6His-*MAD1*$^{529–750}$ by a ribosome-binding site. We generated pET43-6His-*ScMAD2*, pET43-6His-*Scmad2*$^{R126E/Q127A}$, and pET43-6His-*Scmad2*^{ΔC} by replacing the BamHI–EcoRI fragment of pET43-6His-Mad2 (De Antoni et al., 2005a) with coding sequences of *ScMAD2* mutant alleles. The *ScMAD2* HindIII–BglII fragment containing the whole coding region plus ∼400 bp of upstream and ∼280 bp of downstream sequence was cloned in HindIII–BamHI of YIplac128. The resulting pSP42 plasmid was integrated at the *LEU2* locus by EcoRV digestion. *GAL1-MAD2* and *GAL1-mad2ΔC* fusions as well as a *mad2ΔC* allele under the control of ∼400 bp of *MAD2* promoter were cloned in YIplac128 upstream of ∼280 bp of *MAD2* terminator to generate pSP187, pSP385, and pSP384 plasmids, whose integration was directed to the *LEU2* locus by EcoRV digestion. Single integrations were checked by Southern analysis. Mutant alleles were generated using QuikChange (Stratagene). *MAD1* was tagged with the myc tag immediately before the stop codon by one-step gene tagging (Knop et al., 1999). The *myc18-CDC20* strain has been described previously (Shirayama et al., 1998).

Expression, purification, and AlexaFluor labeling of proteins

ScMad2–6His-ScMad1$^{529–750}$ was generated in *Escherichia coli* BL21-c41(DE3). After metal affinity chromatography on a 1-ml HiTrap Chelating HP column (GE Healthcare), the protein was purified by ion exchange on a Resource Q column (GE Healthcare) and dialyzed in buffer L (20 mM Hepes, pH 7.5, 300 mM NaCl, 10% glycerol, and 1 mM EDTA). Mad2 proteins were expressed in *E. coli* BL21(DE3) and purified essentially as described previously for the human complex (Sironi et al., 2001). Proteins were labeled with AlexaFluor488 succimidyl ester reactive dye (Invitrogen) as described previously (Howell et al., 2000), with a final dye/protein ratio of ∼0.5.

Analytical SEC

Analytical SEC was performed on a SMART device (GE Healthcare) using Superdex-75 or -200 PC 3.2/30 columns equilibrated in buffer L. 10 μM

Table I. **Genotypes of *S. cerevisiae*'s strains**

Name	Relevant genotype
ySP581	MATa, *his3-11,15::HIS3::tetR-GFP, ura3::3XURA3::tetO112*
ySP1413	MATa, *myc18-CDC20::TRP1*
ySP2218	MATa *MAD1-myc18::HIS3*
ySP5222	MATa, *mad2::TRP1, his3-11,15::HIS3::tetR-GFP, ura3::3XURA3::tetO112*
ySP5256	MATa, *mad2::TRP1, leu2::LEU2::mad2-R126A, his3-11,15::HIS3::tetR-GFP, ura3::3XURA3::tetO112*
ySP5257	MATa, *mad2::TRP1, leu2::LEU2::mad2-Q127A, his3-11,15::HIS3::tetR-GFP, ura3::3XURA3::tetO112*
ySP5276	MATa, *mad2::TRP1, leu2::LEU2::MAD2, his3-11,15::HIS3::tetR-GFP, ura3::3XURA3::tetO112*
ySP5311	MATa, *mad2::TRP1, leu2::LEU2::MAD2, myc18-CDC20::TRP1*
ySP5314	MATα, *mad2::TRP1, leu2::LEU2::MAD2, MAD1*-myc18::*HIS3*
ySP5316	MATα, *mad2::TRP1, leu2::LEU2::mad2-R126A, MAD1*-myc18::*HIS3*
ySP5318	MATα, *mad2::TRP1, leu2::LEU2::mad2-Q127A, MAD1*-myc18::*HIS3*
ySP5355	MATa, *mad2::TRP1, leu2::LEU2::mad2-R126A, myc18-CDC20::TRP1*
ySP5356	MATa, *mad2::TRP1, leu2::LEU2::mad2-Q127A, myc18-CDC20::TRP1*
ySP5718	MATa, *leu2::LEU2::GAL1-MAD2, his3-11,15::HIS3::tetR-GFP, ura3::3XURA3::tetO112*
ySP5735	MATa, *leu2::LEU2::GAL1-mad2$^{\Delta C}$, his3-11,15::HIS3::tetR-GFP, ura3::3XURA3::tetO112*
ySP5760	MATa, *mad2::TRP1, leu2::LEU2::mad2$^{\Delta C}$, his3-11,15::HIS3::tetR-GFP, ura3::3XURA3::tetO112*
ySP5789	MATa *MAD1-myc18::HIS3, mad2::TRP1, leu2::LEU2::GAL1-mad2$^{\Delta C}$*

of divalent ScMad2–6His-ScMad1$^{529–750}$ complex was incubated for 1 h at 25°C with 20 μM AlexaFluor-ScMad2 or AlexaFluor-ScMad2 mutants. The reactions were separated by SEC. Elution was performed at 40 ml/min. Custom-built synthetic peptides were purchased from Eurogentec.

Protein extracts, IPs, and Western blotting analysis

For IPs, cells were lysed with glass beads in 50 mM Hepes, pH 7.6, 75 mM KCl, 1 mM $MgCl_2$, 1 mM EGTA, 1 mM AEBSF, 0.5 mM DTT, 120 mM β-glycerophosphate, and 0.1% Triton X-100 supplemented with a cocktail of protease inhibitors (Complete; Boehringer). 1–2 mg of cleared extracts was incubated for 2 h with antibody directly cross-linked to protein A–Sepharose, except in the case of the anti-Mad2 IPs. The slurry was washed three times with lysis buffer. Protein extracts were run on 15% SDS-PAGE gels. For Western blot analysis, proteins were transferred to Protran membranes. myc18-Cdc20 and Mad1-myc18 were detected with monoclonal antibody 9E10. Anti-Clb2 polyclonal antibodies were a gift from W. Zachariae (Max Planck Institute of Molecular Cell Biology and Genetics, Dresden, Germany). Anti-ScMad2 polyclonal antibodies used for Fig. 7 A and SF1C were provided by K. Hardwick (Wellcome Trust Centre for Cell Biology, University of Edinburgh, Edinburgh, UK; Hardwick et al., 2000). Anti-ScMad2 polyclonal antibodies used for Fig. 7 (B and C) were produced locally. Secondary antibodies were purchased from GE Healthcare and Bio-Rad Laboratories.

GST-binding assay

GST-ScMad1$^{563–590}$ and GST-ScCdc20$^{184–210}$ were expressed in *E. coli* BL21-c41(DE3). After lysis by sonication in buffer A (10 mM Hepes, pH 7.5, 100 mM NaCl, 1 mM DTT, and 0.5 mM EDTA), 1% Triton X-100 was added. The GST proteins were purified with GSH agarose (GE Healthcare). ∼8 μg GST, GST-ScMad1$^{563–590}$, or GST-ScCdc20$^{184–210}$ on beads were incubated for 1 h at RT with 40 μg ScMad2, ScMad2$^{\Delta C}$, or ScMad2^{RQEA} in 0.3 ml of buffer A (final concentrations of GST fusion protein and Mad2 were ∼1 and ∼5 μM, respectively). Beads were washed twice with 0.4 ml of buffer A supplemented with 1% Triton X-100, and bound proteins were separated by SDS-PAGE.

Flow cytometry and analysis of sister chromatid separation

Flow cytometric DNA quantitation was determined on a FACScan (Becton Dickinson) as described previously (Epstein and Cross, 1992). Sister chromatid separation was followed on ethanol-fixed cells by visualizing tetracycline-repressor GFP fusion proteins bound to tandem repeats of tet operators integrated at ∼35 kb away from the centromere of chromosome V (Michaelis et al., 1997).

Online supplemental material

Fig. S1 shows the characterization of Mad2$^{\Delta C}$ in *S. cerevisiae*. Table S1 provides data on isothermal titration calorimetry. Online supplemental material is available at http://www.jcb.org/cgi/content/full/jcb.200602109/DC1.

We are grateful to W. Zachariae and K. Hardwick for strains and reagents and to K. Nasmyth for support and discussions.

A. De Antoni is a postdoctoral fellow of the Italian Association for Cancer Research and a former EMBO postdoctoral fellow. L. Nezi is supported by the European School of Molecular Medicine. This work was supported by the Italian Association for Cancer Research, the Human Frontier Science Program, and the Fondo di Investimento per la Ricerca di Base. A. Musacchio would like to dedicate this study to Edoardo Musacchio, who was born on February 3, 2006.

Submitted: 17 February 2006
Accepted: 31 May 2006

References

Aravind, L., and E.V. Koonin. 1998. The HORMA domain: a common structural denominator in mitotic checkpoints, chromosome synapsis and DNA repair. *Trends Biochem. Sci.* 23:284–286.

Canman, J.C., E.D. Salmon, and G. Fang. 2002. Inducing precocious anaphase in cultured mammalian cells. *Cell Motil. Cytoskeleton*. 52:61–65.

Chen, R.H., D.M. Brady, D. Smith, A.W. Murray, and K.G. Hardwick. 1999. The spindle checkpoint of budding yeast depends on a tight complex between the Mad1 and Mad2 proteins. *Mol. Biol. Cell*. 10:2607–2618.

Cleveland, D.W., Y. Mao, and K.F. Sullivan. 2003. Centromeres and kinetochores: from epigenetics to mitotic checkpoint signaling. *Cell*. 112:407–421.

De Antoni, A., C.G. Pearson, D. Cimini, J.C. Canman, V. Sala, L. Nezi, M. Mapelli, L. Sironi, M. Faretta, E.D. Salmon, and A. Musacchio. 2005a. The mad1/mad2 complex as a template for mad2 activation in the spindle assembly checkpoint. *Curr. Biol.* 15:214–225.

De Antoni, A., V. Sala, and A. Musacchio. 2005b. Explaining the oligomerization properties of the spindle assembly checkpoint protein Mad2. *Philos. Trans. R. Soc. Lond. B. Biol. Sci.* 360:637–647, discussion 447–448.

Epstein, C.B., and F.R. Cross. 1992. CLB5: a novel B cyclin from budding yeast with a role in S phase. *Genes Dev.* 6:1695–1706.

Fang, G., H. Yu, and M.W. Kirschner. 1998. The checkpoint protein MAD2 and the mitotic regulator CDC20 form a ternary complex with the anaphase-promoting complex to control anaphase initiation. *Genes Dev.* 12:1871–1883.

Habu, T., S.H. Kim, J. Weinstein, and T. Matsumoto. 2002. Identification of a MAD2-binding protein, CMT2, and its role in mitosis. *EMBO J.* 21:6419–6428.

Hagan, R.S., and P.K. Sorger. 2005. Cell biology: the more MAD, the merrier. *Nature*. 434:575–577.

Hardwick, K.G. 2005. Checkpoint signalling: mad2 conformers and signal propagation. *Curr. Biol.* 15:R122–R124.

Hardwick, K.G., R.C. Johnston, D.L. Smith, and A.W. Murray. 2000. MAD3 encodes a novel component of the spindle checkpoint which interacts with Bub3p, Cdc20p, and Mad2p. *J. Cell Biol.* 148:871–882.

Howell, B.J., D.B. Hoffman, G. Fang, A.W. Murray, and E.D. Salmon. 2000. Visualization of Mad2 dynamics at kinetochores, along spindle fibers, and at spindle poles in living cells. *J. Cell Biol.* 150:1233–1250.

Howell, B.J., B. Moree, E.M. Farrar, S. Stewart, G. Fang, and E.D. Salmon. 2004. Spindle checkpoint protein dynamics at kinetochores in living cells. *Curr. Biol.* 14:953–964.

Hwang, L.H., L.F. Lau, D.L. Smith, C.A. Mistrot, K.G. Hardwick, E.S. Hwang, A. Amon, and A.W. Murray. 1998. Budding yeast Cdc20: a target of the spindle checkpoint. *Science*. 279:1041–1044.

Kim, S.H., D.P. Lin, S. Matsumoto, A. Kitazono, and T. Matsumoto. 1998. Fission yeast Slp1: an effector of the Mad2-dependent spindle checkpoint. *Science*. 279:1045–1047.

Knop, M., K. Siegers, G. Pereira, W. Zachariae, B. Winsor, K. Nasmyth, and E. Schiebel. 1999. Epitope tagging of yeast genes using a PCR-based strategy: more tags and improved practical routines. *Yeast*. 15:963–972.

Luo, X., G. Fang, M. Coldiron, Y. Lin, H. Yu, M.W. Kirschner, and G. Wagner. 2000. Structure of the mad2 spindle assembly checkpoint protein and its interaction with cdc20. *Nat. Struct. Biol.* 7:224–229.

Luo, X., Z. Tang, J. Rizo, and H. Yu. 2002. The Mad2 spindle checkpoint protein undergoes similar major conformational changes upon binding to either Mad1 or Cdc20. *Mol. Cell*. 9:59–71.

Luo, X., Z. Tang, G. Xia, K. Wassmann, T. Matsumoto, J. Rizo, and H. Yu. 2004. The Mad2 spindle checkpoint protein has two distinct natively folded states. *Nat. Struct. Mol. Biol.* 11:338–345.

Mapelli, M., F.V. Filipp, G. Rancati, L. Massimiliano, L. Nezi, G. Stier, R.S. Hagan, S. Confalonieri, S. Piatti, M. Sattler, and A. Musacchio. 2006. Determinants of conformational dimerization of Mad2 and its inhibition by p31(comet). *EMBO J.* 25:1273–1284.

Michaelis, C., R. Ciosk, and K. Nasmyth. 1997. Cohesins: chromosomal proteins that prevent premature separation of sister chromatids. *Cell*. 91:35–45.

Musacchio, A., and K.G. Hardwick. 2002. The spindle checkpoint: structural insights into dynamic signalling. *Nat. Rev. Mol. Cell Biol.* 3:731–741.

Nasmyth, K. 2005. How do so few control so many? *Cell*. 120:739–746.

Peters, J.M. 2002. The anaphase-promoting complex: proteolysis in mitosis and beyond. *Mol. Cell*. 9:931–943.

Shah, J.V., E. Botvinick, Z. Bonday, F. Furnari, M. Berns, and D.W. Cleveland. 2004. Dynamics of centromere and kinetochore proteins; implications for checkpoint signaling and silencing. *Curr. Biol.* 14:942–952.

Sherman, F. 2002. Getting started with yeast. *Methods Enzymol.* 350:3–41.

Shirayama, M., W. Zachariae, R. Ciosk, and K. Nasmyth. 1998. The Polo-like kinase Cdc5p and the WD-repeat protein Cdc20p/fizzy are regulators and substrates of the anaphase promoting complex in *Saccharomyces cerevisiae*. *EMBO J.* 17:1336–1349.

Sironi, L., M. Melixetian, M. Faretta, E. Prosperini, K. Helin, and A. Musacchio. 2001. Mad2 binding to Mad1 and Cdc20, rather than oligomerization, is required for the spindle checkpoint. *EMBO J.* 20:6371–6382.

Sironi, L., M. Mapelli, S. Knapp, A.D. Antoni, K.-T. Jeang, and A. Musacchio. 2002. Crystal structure of the tetrameric Mad1-Mad2 core complex: implications of a 'safety belt' binding mechanism for the spindle checkpoint. *EMBO J.* 21:2496–2506.

Vink, M., M. Simonetta, P. Transidico, K. Ferrari, M. Mapelli, A. De Antoni, L. Massimiliano, A. Ciliberto, M. Faretta, E.D. Salmon, and A. Musacchio. 2006. In vitro FRAP identifies the minimal requirements for Mad2 kinetochore dynamics. *Curr. Biol.* 16:755–766.

Xia, G., X. Luo, T. Habu, J. Rizo, T. Matsumoto, and H. Yu. 2004. Conformation-specific binding of p31(comet) antagonizes the function of Mad2 in the spindle checkpoint. *EMBO J.* 23:3133–3143.